Synergistic effects of $CoCl_2$ and ROCK inhibition on mesenchymal stem cell differentiation into neuron-like cells

Emilie Pacary[1], Hélène Legros[1], Samuel Valable[1], Pascal Duchatelle[2], Myriam Lecocq[1], Edwige Petit[1], Olivier Nicole[1] and Myriam Bernaudin[1,*]

[1]UMR-CNRS 6185, Neurodegenerescence: models and therapeutic strategies, University of Caen, CYCERON, Bd Henri Becquerel, BP 5229, 14074 Caen CEDEX, France
[2]CERMN EA3915, Pharmacology and Physiology Department, University of Caen Basse-Normandie, 5 rue Vaubénard, 14032 Caen CEDEX, France
*Author for correspondence (e-mail: bernaudin@cyceron.fr)

Accepted 27 March 2006
Journal of Cell Science 119, 2667-2678 Published by The Company of Biologists 2006
doi:10.1242/jcs.03004

Summary

Bone-marrow-derived mesenchymal stem cells (MSCs) constitute an interesting cellular source to promote brain regeneration after neurodegenerative diseases. Recently, several studies suggested that oxygen-dependent gene expression is of crucial importance in governing the essential steps of neurogenesis such as cell proliferation, survival and differentiation. In this context, we analysed the effect of the HIF-1 (hypoxia inducible factor-1) activation-mimicking agent $CoCl_2$ on MSCs. $CoCl_2$ treatment increased the expression of the anti-proliferative gene *BTG2/PC3* and decreased cyclin D1 expression. Expression of HIF-1α and its target genes *EPO*, *VEGF* and *p21* was also upregulated. These changes were followed by inhibition of cell proliferation and morphological changes resulting in neuron-like cells, which had increased neuronal marker expression and responded to neurotransmitters. Echinomycin, a molecule inhibiting HIF-1 DNA-binding activity, blocked the $CoCl_2$ effect on MSCs. Additionally, by using Y-27632, we demonstrated that Rho kinase (ROCK) inhibition potentiated $CoCl_2$-induced MSC differentiation in particular into dopaminergic neuron-like cells as attested by its effect on tyrosine hydroxylase expression. Altogether, these results support the ability of MSCs to differentiate into neuron-like cells in response to $CoCl_2$, an effect that might act, in part, through HIF-1 activation and cell-cycle arrest, and which is potentiated by inhibition of ROCK.

Supplementary material available online at
http://jcs.biologists.org/cgi/content/full/119/13/2667/DC1

Key words: Cell cycle, Differentiation, HIF-1, Neurogenesis, Rho, Stem cells

Introduction

The discovery of the presence of neural stem cells and neurogenesis in the adult brain, including the human brain, changed the view of the irreparable adult brain and argued for the development of clinical trials for replacing neuronal loss following brain damage. Transplantation of neural stem cells within the adult brain tissue with beneficial effect on functional recovery has been proved in animal models of Parkinson's disease (Studer et al., 1998) and cerebral ischemia (Borlongan et al., 1998). However, their inaccessibility severely limits their potential clinical use. There is growing evidence to suggest that sources of stem cells may reside in several types of adult tissues such as bone marrow (Krause, 2002). These cells may retain the potential to transdifferentiate from one phenotype to another, presenting exciting possibilities for cellular therapies.

Interestingly, in addition to neural stem cells, bone-marrow-derived mesenchymal stem cells (MSCs) may provide an alternative source of neurons. Indeed, in addition to their differentiation into osteoblasts, chondroblasts, adipocytes and hematopoiesis-supporting stromal cells, recent in vitro studies have demonstrated that both human and rodent MSCs have the ability to differentiate into neuron-like cells (Sanchez-Ramos et al., 2000; Sanchez-Ramos, 2002; Woodbury et al., 2000). Moreover, therapeutic benefit has been recently shown in cerebral ischemia (Chen et al., 2001; Kurozumi et al., 2005) and trauma (Mahmood et al., 2001) following administration of these stem cells. However, to date, this cellular plasticity is still controversial and/or seems to be a rare phenomenon (Castro et al., 2002; Long and Yang, 2003; Lu et al., 2004; Neuhuber et al., 2004; Vallieres and Sawchenko, 2003). Only few reports underwent functional assays suggesting that bone-marrow-derived cells differentiated into functional active neurons (Hung et al., 2002; Jiang et al., 2003; Kohyama et al., 2001; Wislet-Gendebien et al., 2005a; Wislet-Gendebien et al., 2005b) and the mechanisms involved in MSC neuronal differentiation are still largely poorly understood.

Recent studies suggest that oxygen-dependent gene expression is of crucial importance in governing essential steps of neurogenesis such as cell proliferation, survival and differentiation. Among the oxygen-sensitive factors, there is the transcriptional factor hypoxia-inducible factor-1 (HIF-1), which consists of two subunits: HIF-1α (120 kDa) and HIF-1β (91-94 kDa). Whereas HIF-1β (ARNT) is expressed constitutively in all cells and does not respond to changes in

oxygen tension, HIF-1α protein, at normal oxygen levels, is rapidly degraded by prolyl-hydroxylase activation. However, under low oxygen levels, HIF-1α protein is stabilized leading to the expression of its target genes such as *EPO* (erythropoietin) and *VEGF* (vascular endothelial growth factor) through hypoxia-responsive elements (HRE) (Sharp and Bernaudin, 2004). Interestingly, it has been demonstrated that low oxygen levels enhance neurogenesis from cerebral progenitors compared with high oxygen levels, an effect that involves EPO (Studer et al., 2000). In addition, VEGF also promotes neurogenesis in vitro and in vivo (Jin et al., 2002; Shingo et al., 2001). However, in contrast to EPO (Jin et al., 2002; Shingo et al., 2001), VEGF may act on neurogenesis by a proliferative effect rather than a differentiating effect on neural stem cells (Cao et al., 2004; Shen et al., 2004).

On the other hand, growing evidence indicates that cell cycle arrest and neurogenesis are highly coordinated and interactive processes, governed by cell-cycle genes and neural transcription factors. In order to differentiate, cells need to leave the cell cycle in G1 and to enter G0 without passing the cell-cycle restriction point. This point is regulated by many molecules such as cyclin-dependent kinases (CDKs), cyclin D family proteins and p53. In neuronal precursors, the anti-proliferative gene *PC3* also named *BTG2/TIS21* is expressed and inhibits cell-cycle progression at the G1 checkpoint by repressing cyclin D1 transcription (Canzoniere et al., 2004). PC3 mRNA is expressed in neuroblasts of the ventricular zone of the neural tube during the last proliferative cycle before differentiation into postmitotic neurons and is therefore a marker for the birth of the neuron (Bradbury et al., 1991). Moreover, its overexpression increases expression of neuronal markers such as Tuj1 (class III β-tubulin) and MAP2 (microtubule-associated protein 2) (Canzoniere et al., 2004).

In addition to the inhibition of cellular proliferation, neuritogenesis, is one of the first steps of neuronal differentiation in which the Rho-ROCK system plays a decisive role (Dickson, 2001; Hall, 1998; Luo, 2000). Activation of the Rho-ROCK pathway leads to inhibition of axonogenesis, whereas its inhibition induces early outgrowth of neurites (Bito et al., 2000; Hirose et al., 1998).

Altogether, these studies underline several major steps and factors in neurogenesis including hypoxic-regulated proteins, the cell cycle and neuritogenesis. To evaluate the involvement of these processes in MSC neuronal differentiation, we have analysed, in mouse MSCs, the effect of $CoCl_2$-induced HIF-1 activation in parallel to cell-cycle gene expression (*PC3/BTG2*, *p21*, *cyclin D1*, *p53*), HIF-1 target gene expression (*EPO*, *VEGF*, *p21*), neuronal marker expression [Tuj1, MAP2, NSE (neuron-specific enolase), NF200 (neurofilament 200) and TH (tyrosine hydroxylase)]. Moreover, we studied the effect of echinomycin, a small molecule that has been shown to inhibit HIF-1 DNA-binding activity, on $CoCl_2$-induced MSC differentiation into neuron-like cells. In addition, we determined the effect of ROCK inhibition, using the drug Y-27632, on $CoCl_2$-induced MSC differentiation. In order to explore the functionality of MSC-derived neuron-like cells, we investigated Ca^{2+} influx in response to neurotransmitters (glutamate, dopamine and serotonin) and electrophysiological properties of $CoCl_2$ and Y-27632 co-treated cells compared with control MSCs.

Results

Characterization of MSCs

Undifferentiated MSCs had a large flat morphology as revealed with phase-contrast microscopy (Fig. 1A) and expressed CD90 and CD44 but not CD31, CD34, CD45, TER119 and CD11b (data not shown), as already reported by others (Bertani et al., 2005; Kopen et al., 1999).

To verify that immunodepleted MSCs were multipotent, we analysed their ability to differentiate into osteocytes and adipocytes using the protocols published by Bertani et al. (Bertani et al., 2005). After 10 days in osteogenic medium or 21 days in adipogenic medium, MSCs differentiated into osteocytes or adipocytes as attested by the increase of alkaline phosphatase (AP) or Oil Red O staining, respectively (supplementary material, Fig. S1).

As the expression of nestin, a neuroectodermal marker, seems to be a prerequisite for acquisition of the capacity to progress towards the neural lineage (Tropepe et al., 2001; Wislet-Gendebien et al., 2003), we studied its expression in undifferentiated MSCs. We showed that 90.7±3.2% of MSCs expressed nestin (Fig. 1C,D). In addition, the neuronal immature marker Tuj1 showed a low level of expression but in 99.1±0.9% of undifferentiated MSCs (Fig. 1C,D). However, the mature neuronal marker MAP2a,b (Fig. 1C) and the astroglial glial fibrillary acidic protein (GFAP) were not detected at the protein level (data not shown).

$CoCl_2$ treatment provoked MSC differentiation into neuron-like cells

We studied the effect of increasing concentrations of $CoCl_2$ (50, 100, 250 and 500 μM) on undifferentiated MSCs and observed a dose-dependent morphological change of the cells (data not shown). Since 250 and 500 μM of $CoCl_2$ appeared to be toxic for these cells, we chose the 100 μM concentration, which was commonly used to mimic HIF-1α activation (Wang et al., 2000) and which induced an increase of EPO mRNA expression in mouse primary neuron and astrocyte cultures (M.B. and E.P., unpublished data).

After 3 days of treatment with 100 μM $CoCl_2$, 83±2% of the cells underwent morphological changes into neuron-like cells (Fig. 1A). Indeed, MSCs differentiated with $CoCl_2$ developed long bipolar branching processes appearing bright under phase-contrast microscopy and particularly visible with the Rhodamine-labelled phalloidin staining (Fig. 1A). No evidence was found to indicate that cell damage and in particular apoptosis occurred during $CoCl_2$ treatment (data not shown).

Interestingly, blockage of protein synthesis with cycloheximide (1 μg/ml) prevented MSCs from adopting neuron-like morphology after $CoCl_2$ application (data not shown) suggesting that morphological changes require new protein synthesis. Importantly, in accordance with a previous study on MSC differentiation into adipocytes, chondrocytes or osteocytes (Pittenger et al., 1999), we observed that MSC differentiation only occurred if cells were plated at appropriate densities ($2.5\text{-}3.0\times10^4$ cells/cm^2) (data not shown). Moreover, serum deprivation induced cell death in both control and $CoCl_2$ conditions and therefore MSC differentiation required serum in the culture medium (supplementary material, Fig. S2).

We also studied nestin whose expression decreases with neuronal maturation (Lendahl et al., 1990). $CoCl_2$ treatment

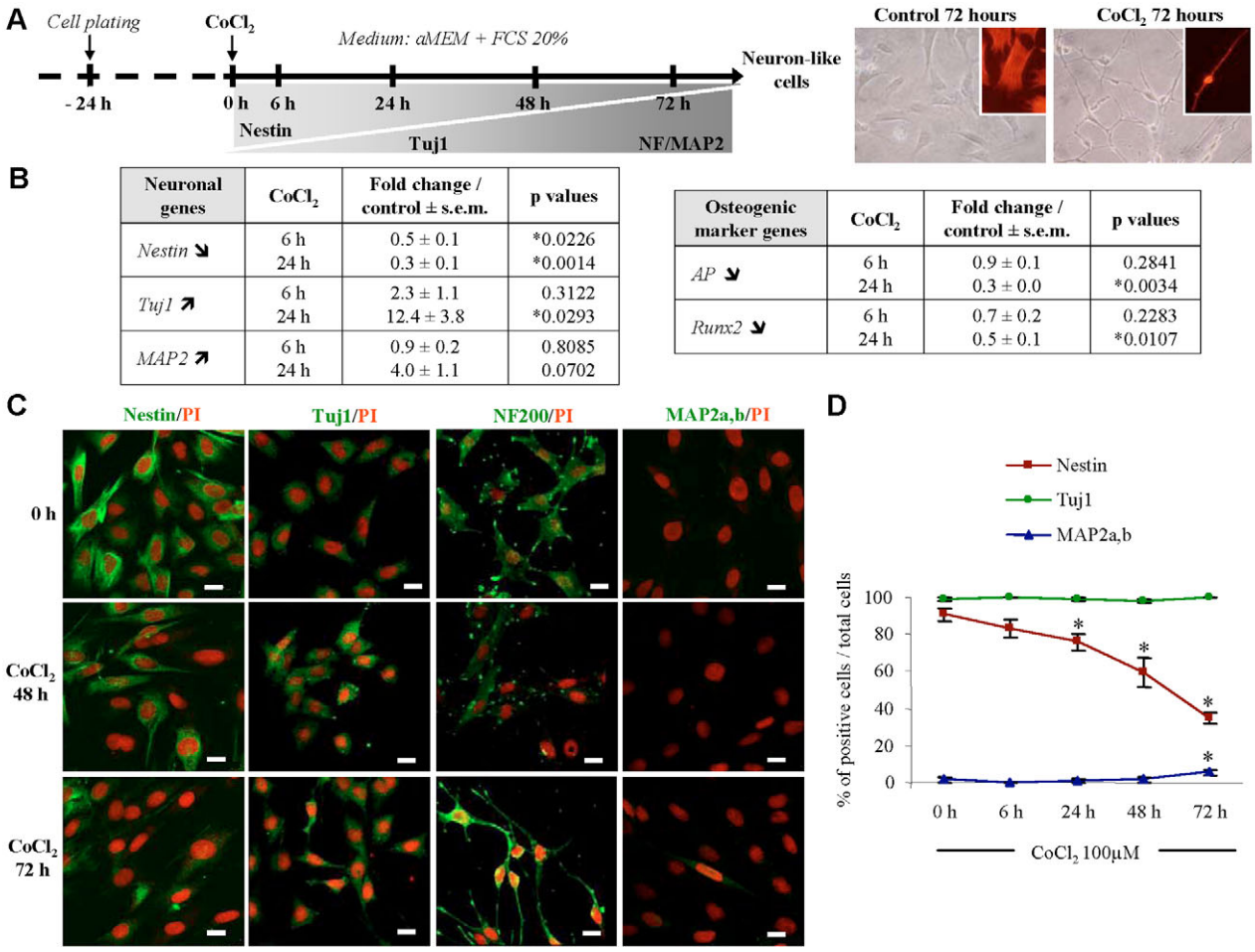

Fig. 1. $CoCl_2$ treatment provoked MSC differentiation into neuron-like cells. (A) MSC morphological changes observed after 72 hours of $CoCl_2$ treatment by phase-contrast microscopy (objective 20×) and by fluorescence microscopy (objective 40×) after Rhodamine-labelled phalloidin staining (insets). (B) Real-time RT-PCR analyses of neuronal genes and osteogenic genes after 6 and 24 hours of $CoCl_2$ treatment. Values are represented as fold change compared with control ± s.e.m., n=3, *P<0.05, univariate Student's t-test. (C) $CoCl_2$-treated cells were stained for neuronal markers (nestin, Tuj1, NF200 and MAP2a,b) and nuclei were counterstained with Propidium Iodide (PI, in red). Photographs were obtained with confocal microscopy. Bars, 20 μm. (D) Quantification of nestin-, Tuj1- and MAP2ab-positive cells compared with total cells during $CoCl_2$ treatment. *P<0.05, Student's t-test, $CoCl_2$-treated cells were compared with control cells.

decreased nestin expression as demonstrated by real-time PCR after 6 and 24 hours of treatment and by immunocytochemistry after 24, 48 and 72 hours of treatment (Fig. 1B-D). In parallel, we performed real-time PCR analyses for two osteogenic markers, *Runx2* (runt-related transcription factor 2) and *ALP* (alkaline phosphatase). As shown in Fig. 1B, $CoCl_2$ treatment significantly decreased *Runx2* and *ALP* mRNA expression at 24 hours (Fig. 1B). In addition, although no significant change of the number of Tuj1-positive cells was observed (Fig. 1D), Tuj1 expression increased at the mRNA level after 24 hours of $CoCl_2$ treatment and at the protein level after 48 and 72 hours (Fig. 1B,C). Moreover, the number of MAP2a,b-positive cells increased after 72 hours of treatment as quantified by immunocytochemistry (Fig. 1C,D). Altogether, these results showed that MSC morphological changes towards neuron-like cells paralleled to a decrease of nestin and osteogenic marker expression whereas an increase in expression of immature (Tuj1) and mature neuronal markers (MAP2a,b and NF200) was observed (Fig. 1).

Finally, we studied the effect of several neurotransmitters (glutamate, dopamine and serotonin) on Ca^{2+} influx into $CoCl_2$-treated MSCs (3 days) compared with undifferentiated MSCs using calcium imaging and therefore intracellular calcium concentration ($[Ca^{2+}]_i$) measurements. $CoCl_2$ increased the number of MSCs responding to dopamine (76±5% for $CoCl_2$-treated cells compared with 20±18% for control cells) and to glutamate (42±9% for $CoCl_2$-treated cells versus 2±2% for control cells). By contrast, serotonin had no effect on $[Ca^{2+}]_i$ (data not shown).

$CoCl_2$ treatment increased expression of HIF-1α and its target genes

We then addressed the question of the potential mechanisms that might explain the $CoCl_2$ effect on MSC differentiation into neuron-like cells. It is well known that $CoCl_2$ is able to mimic HIF-1 activation by hypoxia (Jiang et al., 1997). Accordingly, by using immunological approaches, we evidenced that $CoCl_2$ induced HIF-1α nuclear accumulation and increased its

expression in MSCs as early as 3 hours after treatment (Fig. 2A,B). As hypoxia-activated HIF-1 protein binds to HRE in the promoter and/or enhancers of several genes, we used a HRE-pGL3SV40 construct for a luciferase reporter assay to show that $CoCl_2$ treatment was able to induce HIF-1 activation (Fig. 2F). Moreover, we showed, using real-time PCR, an increase of mRNA expression for several HIF-1 target genes including *EPO*, *VEGF* and *p21*, 6 and/or 24 hours after $CoCl_2$ treatment (Fig. 2C). The increase of HIF-1α expression was sustained at least until 3 days after $CoCl_2$ treatment as shown by immunocytochemistry (Fig. 2A). In addition, western blotting for EPO and VEGF-A showed a slight increase of these proteins at that time (Fig. 2D).

To support a role of HIF-1 in the $CoCl_2$-induced MSC differentiation into neuron-like cells, we also studied the effect of desferroxamine (DFX), another well-known HIF-1 inducer (Wang and Semenza, 1993) on undifferentiated MSCs. We showed that 150 μM DFX provoked, similarly to $CoCl_2$ treatment, an increase of HIF-1 expression in the nucleus after 3 hours, a decrease of nestin, *Runx2* and *ALP* mRNA expression and tended to increase Tuj1 expression after 24 hours of treatment in MSCs (supplementary material, Fig. S3). These gene expression changes were also accompanied by morphological changes of MSCs into bipolar cells after 3-5 days of DFX treatment (supplementary material, Fig. S3). In addition, we used echinomycin, a small molecule previously reported by Kong et al. (Kong et al., 2005) which inhibits HIF-1 DNA-binding activity. Interestingly, we showed that 1.25 nM echinomycin completely blocked the morphological changes induced by $CoCl_2$ (Fig. 2E) along with a decrease of the $CoCl_2$-induced luciferase expression and therefore HIF-1 activation (Fig. 2F).

$CoCl_2$ treatment reduced MSC proliferation and modified cell-cycle gene expression

Growing evidence indicates that cell-cycle arrest and neurogenesis are highly coordinated processes. As the increase of p21 mRNA expression supports a role of $CoCl_2$ in cell-cycle regulation, we next investigated the $CoCl_2$ effect on MSC proliferation and on expression of other genes involved in the cell cycle.

We used BrdU incorporation into nuclei to label dividing S-phase cells. BrdU-positive cells were counted after 6, 24, 48 and 72 hours of $CoCl_2$ treatment. We showed that $CoCl_2$ treatment decreased the number of BrdU-positive MSCs (Fig. 3A,B) and therefore MSC proliferation after 24 hours of treatment i.e. before induction of morphological change (control, 36.5±0.8%; $CoCl_2$, 3.5±0.3%; **P*<0.05, Student's *t*-test). Moreover, after 48 (Fig. 3B) and 72 hours (data not shown) of treatment, $CoCl_2$ completely inhibited MSC proliferation.

To investigate the mechanisms that might mediate the $CoCl_2$-induced inhibition of MSC proliferation, we studied the expression of key genes controlling cell proliferation. Thus, in

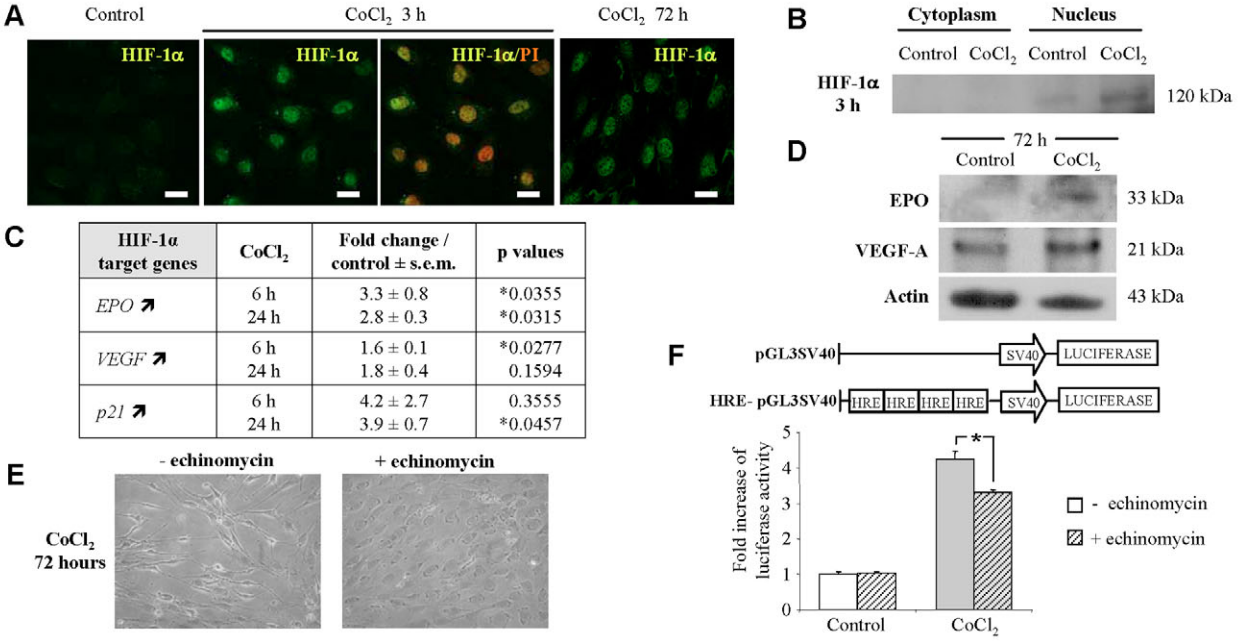

Fig. 2. $CoCl_2$ induced HIF-1α and its target gene expression in MSCs. (A) HIF-1α immunostaining observed in MSCs with confocal microscopy after 3 and 72 hours of 100 μM $CoCl_2$ treatment. In the third image from the left, nuclei were counterstained with Propidium Iodide (PI, in red). Bars, 20 μm. (B) HIF-1α expression analysed by western blotting of cytoplasmic and nuclear extracts from MSCs after 3 hours of $CoCl_2$ treatment. (C) Expression of HIF-1α target genes analysed by real-time RT-PCR after 6 and 24 hours of $CoCl_2$ treatment, n=3, **P*<0.05, univariate Student's *t*-test. (D) Western blot of EPO and VEGF expression after 72 hours of $CoCl_2$ treatment. Actin expression was used as protein loading control. (E) MSC morphology observed after 72 hours of 100 μM $CoCl_2$ treatment with or without 1.25 nM echinomycin (objective 20×). (F) Luciferase activity measurement after 36 hours of 100 μM $CoCl_2$ ± 1.25 nM echinomycin treatment. Firefly luciferase activities were normalized with the internal control *Renilla* luciferase activity. The fold induction represents the luciferase activity observed in transfection with the HRE-pGL3SV40 plasmid relative to the empty plasmid (pGL3SV40). Values are represented as fold induction compared with control ± s.e.m., n=3, **P*<0.05, PLSD Fisher.

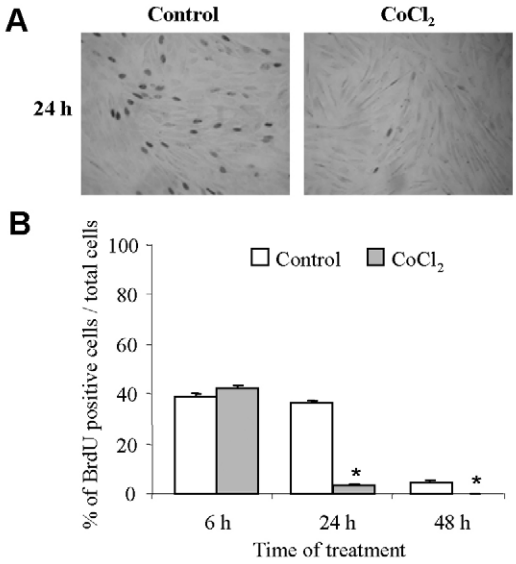

C

Cell cycle genes	$CoCl_2$	Fold change / control ± s.e.m.	p values
p21 ↗	6 h 24 h	4.2 ± 2.7 3.9 ± 0.7	0.3555 *0.0457
BTG2/PC3/TIS21 ↗	6 h 24 h	2.9 ± 1.6 1.8 ± 0.3	0.3145 *0.0472
Cyclin D1 ↘	6 h 24 h	0.4 ± 0.1 0.1 ± 0.1	*0.0100 *0.0099
p53 ↘	6 h 24 h	0.6 ± 0.2 0.5 ± 0.1	0.1015 *0.0372

Fig. 3. $CoCl_2$ decreased MSC proliferation. (A,B) BrdU incorporation of MSCs cultured with or without 100 μM $CoCl_2$. BrdU was incorporated only for the last 2 hours of treatment. (A) BrdU immunostaining using DAB-nickel after 24 hours of treatment. (B) Percentage of BrdU-positive MSCs cultured with or without 100 μM $CoCl_2$ after 6, 24 and 48 hours of treatment. Data shown are mean ± s.e.m. from three independent MSC preparations and from three different wells in each experiment. *P<0.05, Student's t-test, $CoCl_2$-treated cells were compared with control cells. (C) Expression of cell-cycle-related genes was analysed by real-time RT-PCR after 6 and 24 hours of $CoCl_2$ treatment, n=3, *P<0.05, univariate Student's t-test.

parallel to the decrease of BrdU incorporation into cells, we showed an increase of mRNA expression of the anti-proliferative genes *p21* and *PC3/BTG2/TIS21*, which was also correlated with a decrease of cyclin D1 mRNA (Fig. 3C). Cyclin D1, a key cell-cycle regulatory protein that governs cell-cycle progression from the G1 to S phase, was still decreased at the protein level after 3 days of treatment (Fig. 4C). In addition, a significant decrease of p53 mRNA expression was also observed after 24 hours of $CoCl_2$ treatment (Fig. 3C). Altogether these data show that $CoCl_2$ treatment induced cell-cycle arrest of MSCs, a major event in the neuronal differentiation process.

ROCK inhibition potentiated $CoCl_2$-induced MSC differentiation into neuron-like cells

As mentioned above, MSCs differentiated with $CoCl_2$ developed long bipolar processes and appeared bright under phase-contrast microscopy (Fig. 4A,B). A highly controlled balance between elongation and branching is crucial to achieve the ultimate shape of a neuron, which underlines its ability to connect properly to multiple targets. Therefore, our results suggest that MSC differentiation into neuron-like cells induced by $CoCl_2$ is not completely achieved. In addition to the inhibition of cellular proliferation, neuritogenesis, is one of the first steps of neuronal differentiation in which the Rho-ROCK system plays a decisive role (Dickson, 2001; Gallo and Letourneau, 1998; Hall, 1998; Luo, 2000; Narumiya et al., 1997; Nikolic, 2002). We therefore further analysed the ROCK inhibition effect on MSCs treated with $CoCl_2$ or untreated.

When MSCs were treated for 3 days with the ROCK inhibitor Y-27632 (30 μM) alone, no major morphological changes were observed (Fig. 4A,B). However, when MSCs were co-treated for 3 days with $CoCl_2$ and Y-27632, cells more resembled mature neuron-like cells i.e. with small cell bodies but further dendrite-like multipolar processes as shown by phase-contrast microscopy and with Rhodamine-labelled phalloidin staining (Fig. 4A,B). These morphological changes into neuron-like cells, 3 days after $CoCl_2$/Y-27632 treatment, were observed in all clones analysed (n=3) (supplementary material, Fig. S4).

Western blotting analyses showed that Y-27632 did not significantly interfere with the increase of NSE and MAP2c expression and the decrease of cyclin D1 expression induced by $CoCl_2$ (Fig. 4C). More importantly, we showed that co-treatment with both $CoCl_2$ and Y-27632 might potentiate MSC differentiation in particular into dopaminergic neuron-like cells. Indeed, TH expression increased with $CoCl_2$/Y-27632 co-treatment whereas these molecules alone had weak ($CoCl_2$) or no effect (Y-27632) on its expression (Fig. 4D,E).

As expression of neuronal markers does not indicate that these cells are mature functional neurons, we then studied the effect of neurotransmitters on Ca^{2+} influx into $CoCl_2$/Y-27632-treated MSCs (3 days) using a videomicroscopy system and electrophysiological studies. As indicated in Fig. 5, the number of cells responding to dopamine was not significantly changed by $CoCl_2$/Y-27632 co-treatment compared with $CoCl_2$ treatment (Fig. 5A). Nevertheless, we showed that Y-27362, in co-treatment with $CoCl_2$, increased the intensity of the Ca^{2+} influx into MSCs in response to dopamine compared with cells treated with $CoCl_2$ alone whereas Y-27362 alone had no effect (Fig. 5B,C).

Electrophysiological results displayed that in voltage-clamped untreated cells the current-voltage relationship clearly showed an inward rectification for potentials more negative than –80 mV (n=3) (Fig. 6A), an observation consistent with the resting potential measured on these cells which was on

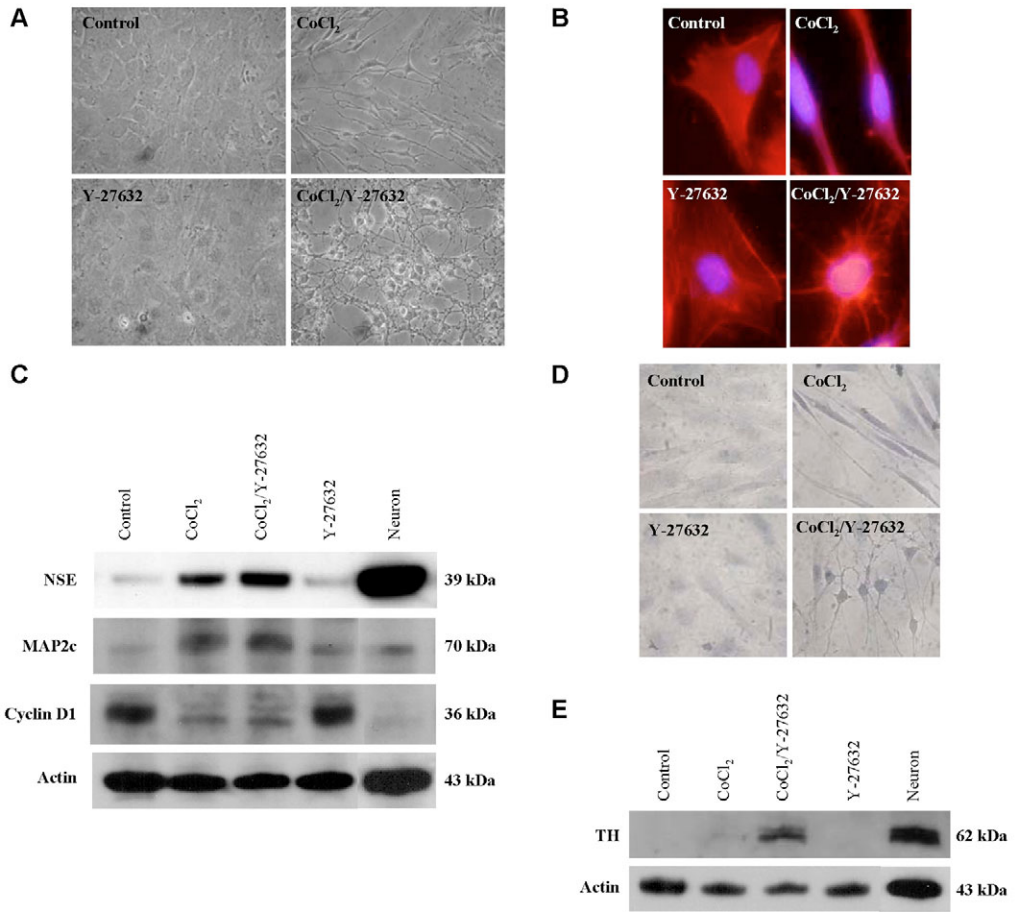

Fig. 4. Y-27632 potentiated $CoCl_2$ effect on MSC differentiation into neuron-like cells. (A,B) MSC morphological changes observed after 72 hours of Y-27632 (30 μM) and/or $CoCl_2$ treatment by phase-contrast microscopy (A) and fluorescence microscopy (B) after Rhodamine-labelled phalloidin staining. (C) Effect of Y-27632 with or without $CoCl_2$ on NSE, MAP2c and cyclin D1 expression, analysed by western blot of MSCs after 72 hours of treatment. Mouse primary-neuron-enriched cultures (11 days in vitro) were used as a positive control and actin was used as protein-loading control. (D,E) TH expression analysed by (D) immunostaining and (E) western blotting after 72 hours of Y-27632 treatment with or without $CoCl_2$.

average –85 mV. However these cells did not show any outward rectifying currents (Fig. 6A). After treatment with both $CoCl_2$ and Y-27632 for 3 days, the resting potential of the cells decreased towards an average value of –36.6±4.6 mV (mean ± s.e.m., n=10). An outwardly rectifying potassium current was recorded and blocked by 10 mM tetraethylammonium (TEA) (n=3) (Fig. 6B). However, we were unable to record tetrodotoxin (TTX)-sensitive inward sodium currents in either control or treated cells.

In order to understand the mechanisms that might explain the potentiating effect of ROCK inhibition on $CoCl_2$-induced MSC differentiation into neuron-like cells and in particular into dopaminergic neuron-like cells, we studied HIF-1α expression in cells treated with $CoCl_2$, $CoCl_2$±Y-27632 or Y-27632 alone compared with untreated cells. We showed by immunocytochemistry (Fig. 7A) and western blot analyses (Fig. 7B), that ROCK inhibition tended to increase the $CoCl_2$-induced increase of HIF-1α expression into the nucleus of MSCs whereas Y-27632 alone had no effect compared with control cells (Fig. 7A,B). Moreover, $CoCl_2$/Y-27632 co-treatment significantly potentiated luciferase expression and therefore HIF-1 activation after 24 and 36 hours of treatment compared with $CoCl_2$ alone (Fig. 7C). Nevertheless, this potentiated effect was not observed at earlier time points (3 and 8 hours of treatment) (Fig. 7C). In accordance with HIF-1α protein expression results (Fig. 7B), Y-27632 alone had no effect on HIF-1 activation compared with control cells (Fig. 7C).

Discussion

Does $CoCl_2$ treatment induce MSC differentiation into neuron-like cells?

Constitutive expression of nestin and Tuj1 by MSCs that we and others (Padovan et al., 2003; Tondreau et al., 2004) observed suggested that these cells have the ability to differentiate into neurons. We hypothesized that HIF-1 activation could trigger MSC differentiation into neuron-like cells. Indeed, HIF-1α and its target genes, *EPO* and *VEGF*, have been shown to be essential for normal development of the brain (Tomita et al., 2003; Yu et al., 2002) and to promote neurogenesis from cerebral progenitors in vitro and in vivo (Csete et al., 2004; Fabel et al., 2003; Jin et al., 2002; Shingo et al., 2001; Sun et al., 2003; Wang, L. et al., 2004; Zhu et al., 2003). This hypothesis has been further supported by recent data (Kotake-Nara et al., 2005) showing that $CoCl_2$, a well-known HIF-1α stabilizer (Jiang et al., 1997), induces neurite outgrowth in PC-12 rat pheochromocytoma cells. Therefore, we investigated the effect of the divalent metal $CoCl_2$ on MSC differentiation.

Interestingly, we showed, for the first time, that MSCs treated with $CoCl_2$ achieved morphology similar to that of neuron-like cells, i.e. long bipolar cells that appeared bright under phase-contrast microscopy with single, long, axon-like developed processes. These morphological changes are accompanied by mRNA and protein expression changes according to a differentiation into neuron-like cells: a decrease

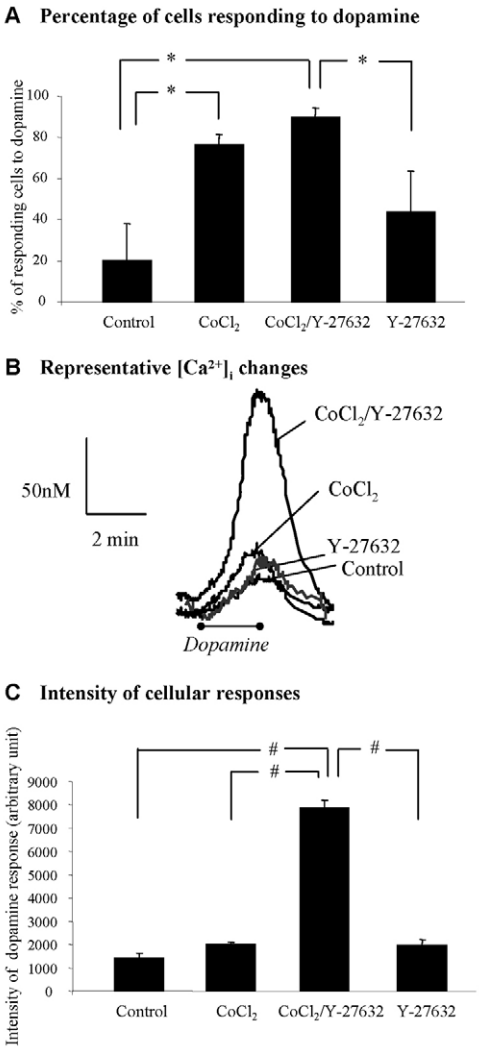

Fig. 5. Effect of 72 hours of $CoCl_2$ and/or Y-27632 treatment on Ca^{2+} influx in response to dopamine in MSCs. (A) Analysis of the percentage of cells responding to dopamine after 72 hours of $CoCl_2$ and/or Y-27632 treatment. *N*=3, *n*=50-75 cells, **P*<0.05, PLSD Fisher. (B,C) Effect of $CoCl_2$ and/or Y-27632 treatment on the intensity of the Ca^{2+} influx in MSCs responding to dopamine. *N*=3, *n*=50-75 cells, **P*<0.05, $^{\#}P$<0.0001, PLSD Fisher.

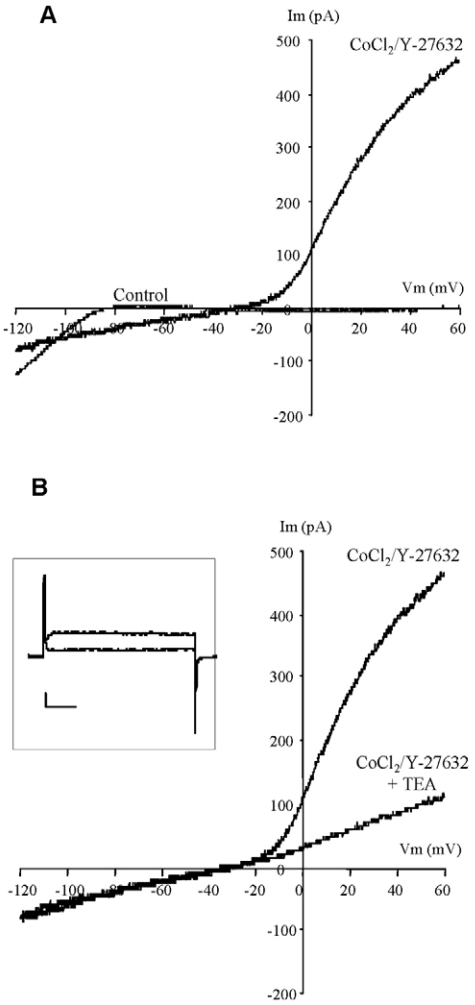

Fig. 6. Electrophysiological properties of control MSCs and $CoCl_2$/Y-27632 co-treated MSCs. Treatment with $CoCl_2$ and Y-27632 induced a change in the currents recorded from MSCs. (A) Control cells showed typical inward-rectifying *I-V* relationship without any sign of voltage-dependent current at depolarizing potentials (*n*=3). Treated cells, by contrast, clearly exhibited outward-rectifying current similar to that found in neurons (*n*=10). (B) The outward-rectifying current encountered in $CoCl_2$/Y-27632 co-treated cells was completely blocked by 10 mM TEA (*n*=3). Insert shows current traces obtained with a voltage step to +60 mV in the presence and absence of 10 mM TEA. Calibration bars, 250 pA 100 milliseconds.

of immature stem cell marker (nestin) along with an increase of neuronal immature marker (Tuj1) and thereafter of more mature neuronal markers (MAP2a,b,c, NF200 and NSE) in parallel to a decrease of osteogenic markers (Runx2 and AP). Our observations are in accordance with the results published by Salim et al. (Salim et al., 2004) showing that anoxia inhibits osteogenic differentiation and Runx2 expression in primary osteoblasts and human bone-marrow-derived mesenchymal cells. These results are also agree with the decrease of *ALP* and Runx2 expression in human bone-marrow-derived neural stem-like cells (Hermann et al., 2004). Moreover, the decrease of nestin expression, which is consistent with ongoing maturation, was also observed with the protocol of MSC differentiation used by Woodbury and colleagues, except that with this protocol there was first an increase after 5 hours and then a decrease (Woodbury et al., 2000). Our results differ from those of Lu et al. (Lu et al., 2004) who did not show any nestin and Tuj1 expression changes using RT-PCR; we observed such changes by both RT-PCR and immunocytochemistry. Although MAP2c is not specific to neuronal cells, the increase of this isoform by $CoCl_2$ treatment in MSCs is of particular interest. Indeed, this isoform is highly expressed during all stages of neuromorphogenesis and might be involved in neurite initiation (Dehmelt et al., 2003). But importantly, as NSE and MAP2c are also expressed in astrocytes and/or oligodendrocytes (Deloulme et al., 1996; Sensenbrenner et al., 1997), studies aiming to demonstrate the existence of functional neuron-like cells are of real importance. We

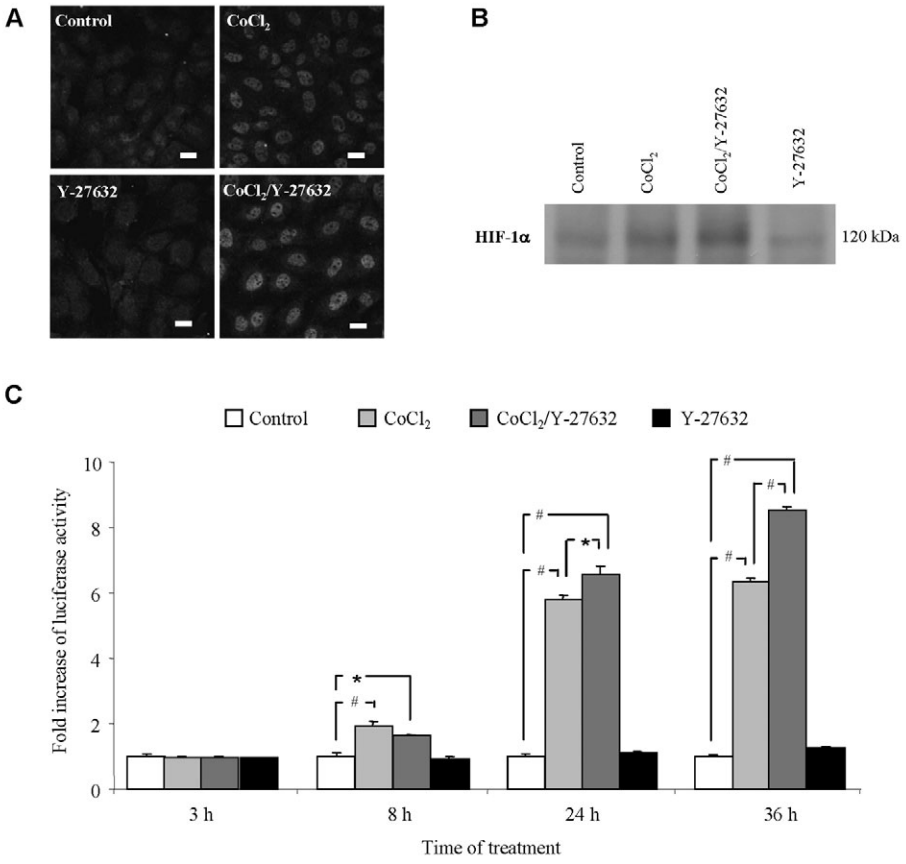

Fig. 7. Effect of Y-27632 on HIF-1α expression in MSCs with or without $CoCl_2$ treatment. (A) HIF-1α immunostaining observed with confocal microscopy on MSCs treated with $CoCl_2$ and/or Y-27632 for 3 hours. Bar, 20 μm. (B) HIF-1α western blot performed from nuclear extracts after 3 hours of $CoCl_2$ and/or Y-27632 treatment. (C) Luciferase activity measurement after 3, 8, 24 and 36 hours of $CoCl_2$ and/or Y-27632 treatment. Firefly luciferase activities were normalized with the internal control *Renilla* luciferase activity. The fold induction represents the luciferase activity observed in transfection with the HRE-pGL3SV40 plasmid relative to the empty plasmid (pGL3SV40). The values are represented as fold induction compared with control ± s.e.m., n=3, $^{*}P$<0.05, $^{\#}P$<0.0001, PLSD Fisher.

therefore studied, using calcium videomicroscopy, the response of MSCs to several neurotransmitters (glutamate, dopamine and serotonin) after 3 days of $CoCl_2$ treatment and revealed that more cells respond to glutamate (42%) and dopamine (76%) but not to serotonin compared with control cells. These improved responses to neurotransmitters strongly support MSC differentiation into neuron-like cells and suggest that these phenotypic changes do not correspond to cellular toxicity or solely cell shrinkage as suggested by others (Lu et al., 2004; Neuhuber et al., 2004).

Could $CoCl_2$-induced MSC differentiation into neuron-like cells be further enhanced with neuritogenic factors?

To study the effect of the Rho-ROCK system, which is known to play a role in neuritogenesis, on MSC neuronal differentiation (Dickson, 2001; Hall, 1998; Luo, 2000), we examined the effect of ROCK inhibition, using Y-27632, on MSCs treated or not with $CoCl_2$. We showed, for the first time, that Y-27632 potentiated the MSC differentiation induced by $CoCl_2$ particularly towards dopaminergic neuron-like cells. Indeed, Y-27632 in co-treatment with $CoCl_2$ dramatically increased TH expression in parallel to profound changes in morphology and cytoskeleton organization. These results are in accordance with those published on neuronal cell lines and primary neuronal cultures showing that Rho induces neurite retraction and conversely Rho inactivation enhances neurite extension and growth cone movement (Bito et al., 2000; Hirose et al., 1998).

The videomicroscopy and electrophysiological results showed that MSCs co-treated for 3 days with $CoCl_2$ and Y-27632 presented potentiated dopamine responsiveness and voltage-gated K^+ currents inhibited by TEA but no voltage-gated Na^+ currents. Although these results do not show truly functional neurons, they are in accordance with those recently published by Wislet-Gendebien et al. (Wislet-Gendebien et al., 2005b). Indeed, these authors showed that at 4-6 days of culture, MSCs co-cultured with cerebellar granule neurons present exactly the same characteristics, i.e. some neurotransmitter responsiveness, voltage-gated K^+ currents inhibited by TEA and that voltage-gated Na^+ currents inhibited by TTX appeared only around 1 week of culture. Therefore, future experiments will be necessary to characterize the long-term effect of $CoCl_2$ and Y-27632 co-treatment on MSC differentiation into neuron-like cells and in particular, as reported by Wislet-Gendebien et al. (Wislet-Gendebien et al., 2005b), to determine whether these cells exhibit other important criteria such as action potentials, synapses with other neurons, neurotransmitter release and receptors.

What mechanisms induced by $CoCl_2$ and Y-27632 treatment might explain MSC differentiation into neuron-like cells?

Interestingly, media containing low or no serum did not induce MSC morphological changes suggesting that $CoCl_2$ differentiation required factors present in the serum (data not shown). These results are in accordance with those of Padovan et al. (Padovan et al., 2003) showing the influence of fetal bovine serum for neuronal differentiation in the presence of FGF-2. Alternatively, this can be explained by the fact that cell death induced by serum deprivation in both control and $CoCl_2$-

treated cells might have prevented MSC differentiation. Moreover, in contrast to the rapid (3 hours) 'Woodbury differentiating protocol' (Woodbury et al., 2000), the morphological changes occurred after 3 days of $CoCl_2$ treatment supporting the need of protein synthesis. This hypothesis was further supported by our results showing that cycloheximide prevented $CoCl_2$-induced MSC differentiation into neuron-like cells.

The present study revealed that HIF-1 activation and expression of its target genes such as *EPO, VEGF* and *p21* might participate in $CoCl_2$-induced MSC differentiation into neuron-like cells. In accordance with this hypothesis, we showed similar results using DFX, another well-known pharmacological inducer of HIF-1 (Wang and Semenza, 1993), i.e. morphological changes, decrease of nestin, *Runx2* and *ALP* mRNA expression along with a tendency to increase Tuj1 mRNA expression. More importantly, we showed that echinomycin, a small molecule inhibiting HIF-1 DNA-binding activity (Kong et al., 2005) completely blocked the morphological changes induced by $CoCl_2$ along with a decrease of HIF-1 activation. Altogether, these results support a potential role of HIF-1 in $CoCl_2$-induced MSC differentiation into neuron-like cells. However, it is important to point out that these studies did not provide direct proof of a role for HIF-1 in the $CoCl_2$-induced MSC differentiation into neuron-like cells and that HIF-1 activation may not represent the only mechanism responsible for this effect.

The increases in $CoCl_2$-induced HIF-1-responsive gene expression in MSCs are modest (two- to fourfold increase for *EPO*, *VEGF* or *p21*) compared with that observed in other cell types such as hepatocytes and kidney cells. Interestingly, Salim et al. (Salim et al., 2004) observed similar changes of around three- to fourfold for *VEGF* and *ADM* (adrenomedullin) (another known HIF-1 target gene) in MSCs subjected to 0.02% O_2 for 24 hours. Therefore, there might be no significant difference between $CoCl_2$ and hypoxia responses on HIF-1 target gene expression but rather a difference depending on the cell type.

The increase of p21 mRNA expression supported an effect of $CoCl_2$ on cell-cycle regulation. Indeed, at high concentrations, p21 robustly inhibits CDK activity, which induces exit from the cell cycle in G0 (Harper et al., 1993; Xiong et al., 1993). Therefore, we investigated the effect of $CoCl_2$ on MSC proliferation and on the expression of other genes involved in the cell cycle. We showed an increase of the anti-proliferative gene *PC3/BTG2/TIS21* along with a decrease of cyclin D1 expression. A mutually exclusive interaction of PC3 and cyclin D1 has been reported previously: cyclin D1 blocked the effects of PC3 on the cell cycle and PC3 inhibited cyclin D1 expression (Canzoniere et al., 2004; Guardavaccaro et al., 2000). A significant decrease of p53 mRNA expression was also observed after 24 hours of $CoCl_2$ treatment. This transcriptional repression of *p53* by $CoCl_2$ has been reported by Lee et al. (Lee et al., 2001) in HeLa cells. Of note, in $CoCl_2$-treated cells, the proliferation rate decreased as early as 24 hours after treatment to completely stop at 48 hours. Therefore, increases in neuronal marker expression cannot be related to an increase in the number of cells.

Altogether, our results are in accordance with a potential role of the transcription factor HIF-1 and cell-cycle arrest in the differentiation of MSCs into neuron-like cells. Indeed, HIF-1 has been shown to be essential for cell-cycle arrest during hypoxia. For example, Goda et al. (Goda et al., 2003) showed that hypoxia causes a HIF-1-dependent increase in the expression of the cyclin-dependent kinase inhibitors p21 and p27 in murine embryonic fibroblasts and splenic B lymphocytes. Therefore, our findings, along with those published in the literature, reflect a $CoCl_2$-induced growth arrest in MSCs that might be induced by HIF-1 activation.

Concerning the potentiated effect of ROCK inhibition on $CoCl_2$-induced MSC differentiation into neuron-like cells, an obvious mechanism is cytoskeleton modification, a well-known effect of Rho-ROCK pathways as discussed above. In addition, neurite outgrowth has been linked to the arrest of cell division. Although differentiation may cause changes in cell shape, several studies have noted that changes in cell shape themselves can alter the differentiation of precommitted mesenchymal lineages (McBeath et al., 2004). RhoA might convey the 'cell-shape signal' to the cell-cycle machinery by, for example, promoting G1 progression by altering the balance between ROCK and mDia1 (Mammoto et al., 2004) or increasing activation of cyclin D1 transcription as shown on chondrocytes (Wang, G. et al., 2004). However, in the present study, we showed that ROCK inhibition with Y-27632 did not further decrease cyclin D1 expression induced by $CoCl_2$. Moreover, Y-27632 alone did not have an effect on either cell morphology or on cyclin D1 expression suggesting that other mechanisms might be implicated. In addition, Y-27632 alone did not have effect on HIF-1α expression. Nevertheless, in association with $CoCl_2$, Y-27632 further increased HIF-1α expression into the nucleus and HIF-1 activation. This is the first report of an effect of Rho-ROCK inhibition on HIF-1 and this effect may account, at least in part, for the effect of Y-27632 on $CoCl_2$-induced MSC differentiation into neuron-like cells. Therefore, further investigations on the potential ROCK/HIF-1 relationship appear of importance to determine the precise mechanisms implicated in this effect.

In conclusion, these results support the ability of MSCs to differentiate into neuron-like cells in response to $CoCl_2$ and Y-27632, an effect that might act through, at least in part, HIF-1 activation, cell-cycle arrest and ROCK inhibition. These results are in accordance with those previously published reporting an effect of $CoCl_2$ on the differentiation of several cell types including PC12 cells, an effect linked to HIF-1, p53 and p21 expression (Huang et al., 2003; Kotake-Nara et al., 2005; Wang et al., 2000). $CoCl_2$ treatment was chosen in this study to mimic hypoxia-induced HIF-1 activation. However, potential differences between $CoCl_2$ treatment and hypoxia incubation may be expected and further experiments will be necessary to determine these. Indeed, one might expect that hypoxia induces many other transcriptional factors and genes that are not induced by $CoCl_2$, because in addition to HIF-1, other proteins such as EGR-1 (early growth response-1), MTF-1 (metal transcription factor-1), NF-IL6 (nuclear factor interleukin-6), as well as NF-kappa B (which may also have a role in neuronal differentiation), are all induced by hypoxia (Semenza, 2000; Sharp and Bernaudin, 2004).

Altogether these data support MSCs as a source of neurons and revealed that Y-27632 in co-treatment with $CoCl_2$ might be a useful paradigm to differentiate MSCs into dopaminergic

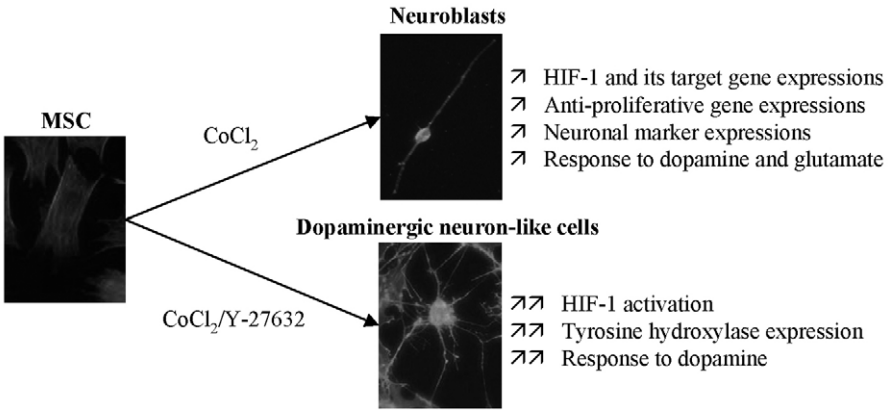

Fig. 8. Schematic representation of the effect of $CoCl_2$ and Y-27632 treatments on MSC differentiation in neuron-like cells. Images of MSC morphology were obtained after Rhodamine-labelled phalloidin staining and observed by fluorescence microscopy. One arrow indicates an increase and two arrows, a larger increase.

neuron-like cells (Fig. 8). Therefore, this study, by contributing to a better understanding of the potential differentiation of MSCs into neurons, should help the development of cellular and genetic therapy protocols and provide new perspectives in the field of adult stem cell research and brain disorders.

Materials and Methods

Purification of MSCs

MSCs were purified as previously described by Kopen et al. (Kopen et al., 1999) who developed a reliable method to eliminate myelopoietic unwanted cells expressing CD11b, which particularly adhered in mouse MSC preparation. Bone marrow cells were extracted from femurs and tibias of adult male mice (Swiss, 8 weeks old) by flushing bones with αMEM (Eagle's minimal essential medium; Eurobio, France) and cultured in this medium supplemented with 20% FCS (fetal calf serum) and 2 mM glutamine. After 2 passages, cells were resuspended in a separation buffer [phosphate-buffered saline (PBS), EDTA 2 mM, 0.5% bovine serum albumin (BSA), pH 7.2] supplemented with biotinylated CD11b antibody (0.5 mg/ml; BD Biosciences, France). After 1 hour of incubation at 4°C, cells were incubated with streptavidin-coated paramagnetic beads (MACS Streptavidin Microbeads, Miltenyi Biotec, France) for 15 minutes at 4°C and centrifuged 10 minutes at 300 ***g***. Thereafter, the pellet was resuspended in separation buffer and cell suspension was put on a column fixed on a magnetic support (Miltenyi Biotec). Cells not bound to the beads, i.e. those that do not express CD11b (MSCs), were harvested, washed and resuspended in αMEM with serum and glutamine.

Osteogenic and adipogenic differentiation of MSCs

Osteogenic and adipogenic differentiation of MSCs were induced according to a protocol published by Bertani et al. (Bertani et al., 2005). For osteogenic differentiation, cells were seeded at a density of 3×10^3 cells/cm^2 and cultured for 10 days with 100 nM dexamethasone, 50 μM ascorbic acid and 10 mM β-glycerophosphate. Osteoblast differentiation was evaluated by alkaline phosphatase (AP) staining (Sigma, France) according to the manufacturer's protocol. To achieve adipogenic differentiation, cells were grown in the presence of 1 μM dexamethasone, 0.2 mM indomethacin, 10 μg/ml insulin and 0.5 mM 3-isobutyl-1-methylxanthine. After 3 weeks of culture, cells were fixed with 4% paraformaldehyde, covered with 3 mg/ml Oil Red O (Sigma) dissolved in 60% isopropanol for 10 minutes and the excess dye was washed out with water.

Clonal analysis of MSCs

MSCs were serially diluted into αMEM with 20% FCS and 2 mM glutamine in 96-well plates. Only single cells were expanded with MSC culture medium for additional 2 weeks. When the appropriate number of cells was achieved, cells were treated using the neuronal induction protocol described below.

Neuronal differentiation of MSCs

To initiate neuronal differentiation, subconfluent MSCs were treated with 100 μM $CoCl_2$ (Sigma) and/or 30 μM Y-27632 (Calbiochem, France) supplemented to the medium. Both $CoCl_2$ and Y-27632 were added at the same time for the same duration. Subconfluent MSCs were also treated with 150 μM desferroxamine (DFX) (Sigma) or 1.25 nM echinomycin (Sigma) supplemented to the medium. As Y-27632 and echinomycin were resuspended in dimethyl sulfoxide (DMSO), control cells were also treated with 0.3% DMSO or 0.125% DMSO, respectively.

Rhodamine-labelled phalloidin and Hoechst 33342 staining

Cells were fixed with 4% paraformaldehyde (pH 7.4) for 10 minutes and rinsed with PBS. The cells were then permeabilized with 0.1% Triton X-100-PBS, incubated with Rhodamine-labelled phalloidin (10 μg/ml) (Sigma) for 40 minutes and rinsed in PBS. Thereafter, cells were incubated with Hoechst 33342 (10 μg/ml, Sigma) for 15 minutes and rinsed again in PBS.

RNA isolation

Total RNAs were collected by scraping MSCs with TRIzol® reagent (Invitrogen Life Technologies, France) according to the manufacturer's protocol. After extraction with chloroform (an additional step of phenol/chloroform extraction is added to the manufacturer's protocol), RNAs were precipitated by isopropyl alcohol. The quality and quantity of total extracted RNA samples were then examined using spectrophotometric OD_{260} and OD_{280} measurements.

Quantitative real-time RT- PCR

1 μg of total RNA from each sample was reverse-transcribed using the Promega RT system (Promega, France) (RT at 42°C for 1 hour). 2-3 μl RT product were then used for PCR amplification in a total volume of 25 μl. Forward (F) and reverse (R) primers were designed for each gene using Beacon Designer software (BioRad, France): *ALP* (116 bp), F 5′-GTGAGCGACACGGACAAGAAG-3′ and R 5′-TTGTTGTGAGCGTAATCTACCATG-3′; *BTG2/PC3/TIS21* (118 bp), F 5′-CCGTCATCATCGTTCTAATACAGC-3′ and R 5′-CCTCAGGAGACTGGAGAGGAAA-3′; *Cyclin D1* (149 bp), F 5′-TTCCAGAGTCATCAAGTGTGACC-3′ and R 5′-GACCAGCCTCTTCCTCCACT-3′; *EPO* (108 bp), F 5′-AGCTCAGAAGGAATTGATGTCGC-3′ and R 5′-AGGAAGTTGGCGTAGACCCG-3′; *MAP2* (120 bp), F 5′-CAGACTTCCACCGAGCAGTCT-3′ and R 5′-GGCTGCATCTGTAACTGCTTGTT-3′; *Nestin* (113 bp), F 5′-GAGAAGACAGTGAGGCAGATGAGTTA-3′ and R 5′-GCCTCTGTTCTCCAGCTTGCT-3′; *p21* (96 bp), F 5′-CGAGAACGGTGGAACTTTGACTT-3′ and R 5′-GTAGACCTTGGGCAGCCCTAG-3′; *p53* (119 bp), F 5′-GGACAGCTTTGAGGTTCGTGTT-3′ and R 5′-CTCTCTTTGCGCTCCCTGGG-3′; *Runx2* (143 bp), F 5′-TCTGAGCCAGATGACATCCCC-3′ and R 5′-AAGGCCAGAGGCAGAAGTCA-3′; *Tuj1* (91 bp), F 5′-GGCGCCTTTGGACACCTATT-3′ and R 5′-CCTCCGTATAGTGCCCTTTGG-3′; *VEGF-A* (130 bp), F 5′-AAATCACTGTGAGCCTTGTTCAG-3′ and R 5′-GCTGCCTCGCCTTGCA-3′. Assays were run in duplicate on the iCycler iQ™ real-time PCR detection system (Biorad). The amplification profile was as follows: Hot Goldstar enzyme activation, 95°C for 3 minutes; PCR 50 cycles at 95°C, 15 seconds and 60°C, 1 minute. The PCR was done according to the manufacturer's protocol using the qPCR™ Core Kit Sybr™ Green I – No Rox (Eurogentec, France). The results were analysed using a comparative method after having confirmed that PCR efficiencies were between 90 and 110%. The amount of target is given by the formula 2^{-Ct}, where *C*t represents the threshold cycle, indicating the fractional cycle number at which the amount of amplified target reaches a fixed threshold.

Immunocytochemistry

After washing in PBS, cells were fixed with 4% paraformaldehyde (pH 7.4) for 10 minutes and rinsed again with PBS. The cells were permeabilized with 0.1% Tween-PBS or 0.5% Triton X-100-PBS (for HIF-1 analysis) for 5 minutes and treated with 3% BSA-0.1% Tween-PBS or 10% FCS-PBS (for HIF-1 analysis) for 30 minutes. Thereafter they were incubated overnight at 4°C with the primary antibody (anti-CD11b, BD Biosciences, 2.5 μg/ml; anti-nestin, Chemicon, France, 5.1 μg/ml; anti-Tuj1, Chemicon, 10-25 μg/ml; anti-NF200, Sigma, 83 μg/ml; anti-MAP2a,b, Sigma, 20 μg/ml; anti-HIF-1α, 100-105 Abcam Novus-Biologicals, France, 0.4 μg/ml; anti-TH, Chemicon, 0.01-0.025 μg/ml) in 1% BSA-PBS. Cells were then incubated for 1.5 hours with FITC-conjugated goat anti-mouse, FITC-conjugated goat anti-rabbit (Molecular Probes, The Netherlands), anti-mouse biotinylated (Sigma) or anti-rat biotinylated antibody (Vector, USA). The fluorescence was visualized using confocal microscopy (Nikon). For some markers, images were

revealed after 2 hours of incubation with peroxidase streptavidin (Sigma) and diaminobenzidine (Vector).

Preparation of total, cytosolic and nuclear protein extracts

For total protein extracts, cells were lysed with TNT buffer (50 mM Tris-HCl, 150 mM NaCl, 0.5% Triton X-100, pH 7.4; Sigma) supplemented with 1 μg/ml protease inhibitors. For cellular cytosolic and nuclear protein extracts, cells were first lysed with buffer A (20 mM HEPES, 10 mM KCl, 1 mM EDTA, 1 mM dithiothreitol, 0.2% NP40, 10% glycerol, 1 mM PMSF, 0.1 mM sodium orthovanadate and 1 μg/ml protease inhibitors in distilled water; Sigma). After 5 minutes on ice, samples were centrifuged for 10 minutes at 13,000 ***g***. Supernatants (cytosolic extracts) were kept at –20°C. Pellets were resuspended in buffer B (350 mM NaCl, 20% glycerol, 20 mM HEPES, 10 mM KCl, 1 mM EDTA, 1 mM PMSF, 0.1 mM vanadate and 1 μg/ml protease inhibitors in distilled water; Sigma). Suspension was mixed vigorously and incubated on ice for 30 minutes. Then, samples were centrifuged for 10 minutes at 13,000 ***g*** and supernatants (nuclear extracts) were kept at –20°C.

Western blot analyses

For HIF-1α western blot analysis, after separation by 7.5% SDS-polyacrylamide gel electrophoresis (PAGE), proteins (70 μg) were transferred to polyvinylidene difluoride (PDVF) membranes (PerkinElmer-NEN, France). Then membranes were blocked for 1 hour in 5% non-fat milk in Tris-buffered saline (TBS) containing 0.05% Tween 20 (T-TBS) and incubated with the antibody overnight at 4°C (7.25 μg/ml; Abcam Novus-Biologicals 100-105). After washing in T-TBS, membranes were incubated for 1 hour at room temperature with peroxidase-labelled secondary antibodies. The immunoreactive bands were visualized by enhanced chemiluminescence (PerkinElmer-NEN).

For other western blot analyses, proteins (50 μg) were separated on 4-12% gradient gels using the XCell Surelock Mini-Cell and the NuPAGE® MES SDS Running Buffer (Invitrogen Life technologies) according to the manufacturer's protocol. Proteins were then transferred using the XCell II Blot Module and the NuPAGE® Transfer Buffer (Invitrogen Life technologies). Membranes were treated as described above. Concentrations of primary antibodies were as follows: NSE (4-6 μg/ml, Chemicon); MAP2a,b,c (19.4 μg/ml, Sigma); TH (0.08 μg/ml, Chemicon); EPO (2 μg/ml, Sigma); VEGF (1 μg/ml, Santa Cruz, USA); cyclin D1 (3 μg/ml, Cell Signaling Technology, USA) and actin (0.8 μg/ml, Sigma). The immunoblot photographs were representative of three independent experiments.

Luciferase assay

HRE-pGL3SV40-luciferase construct was kindly provided by Prof. Soubrier (from INSERM U525, Paris, France) (Coulet et al., 2003). Using Amaxa nucleofection technology™ (Amaxa, Germany), cells were transfected with 2 μg luciferase construct [HRE-pGL3SV40-luciferase or pGL3SV40-luciferase (Promega) constructs] and pRL-TK plasmid, which contained a herpes simplex virus thymidine kinase promoter upstream of the *Renilla* luciferase gene. After 16 hours of culture, cells were treated with $CoCl_2$ and/or echinomycin or with $CoCl_2$ and/or Y-27632. Cells were then washed with PBS, and lysed with Passive lysis buffer (Promega). Firefly luciferase and *Renilla* luciferase activities were measured sequentially by using a Dual-Luciferase Reporter assay system (Promega) and a luminometer (Turner Designs, USA). After measuring the firefly luciferase signal (FLS) and the *Renilla* luciferase signal (RLS), we calculated the relative luciferase activity as FLS/RLS.

Bromodeoxyuridine incorporation and labelling

Bromodeoxyuridine (BrdU; Sigma) (30 μM) was included for the last 2 hours of $CoCl_2$ application. After 6, 24, 48 and 72 hours of $CoCl_2$ treatment, cells were fixed with 4% paraformaldehyde and rinsed in PBS. Cells were then heated 2 hours at 65°C in 50% formamide in 2× SSC, treated 30 minutes in 2 N HCl at 37°C and the reaction was neutralized in 0.1 M boric acid (pH 8.5) for 10 minutes (Sigma). Thereafter, the cells were washed in PBS, incubated 20 minutes in 3% H_2O_2 in PBS and washed again in PBS. After blocking the non-specific bindings 30 minutes with PBS/3% BSA/0.3% Triton X-100, cells were incubated overnight with anti-BrdU antibody (5.5 μg/ml, Chemicon) diluted in PBS/3% BSA/0.3% Triton X-100. Primary antibody was detected by incubation with anti-mouse biotinylated antibody (Sigma) diluted in PBS/3% BSA/0.3% Triton X-100 for 2 hours. Staining was visualized after 2 hours of incubation in an avidin-biotin complex prepared in PBS/0.3% Triton X-100 (Vector) with diaminobenzidine-nickel (Vector).

Calcium imaging

Cell cultures were loaded for 45 minutes in a HEPES-buffered saline solution containing 5 μM Fura-2/AM plus 0.01% pluronic F-127 (Molecular Probes). Experiments were performed at room temperature, on the stage of a Nikon Eclipse inverted microscope equipped with a 75W Xenon lamp and a Nikon 40×/1.3 NA epifluoresence oil-immersion objective. Fura-2 (excitation: 340, 380 nm; emission: 510 nm) ratio images were acquired with a CDD camera and digitized (256×512 pixels) using Metafluor 4.11 software (Universal Imaging Corporation, USA). Each neurotransmitter (500 μM; glutamate, dopamine, serotonin; Sigma) was applied 2 minutes and ATP (100 μM; Sigma) was used as a positive control and applied for 30 seconds. The cells were considered as responding cells when neurotransmitters induced an increase of at least 20% in Ca^{2+} influx compared with the basal level. The intensity of the Ca^{2+} influx was evaluated by measuring the area under the curve.

Electrophysiology

Cells were cultured on glass coverslips (Esco, Erie Scientific Company, USA) and were voltage-clamped with standard whole-cell patch-clamp methods (Hamill et al., 1981) under the stage of an inverted microscope. The normal extracellular bathing solution contained 140 mM NaCl, 3.5 mM KCl, 2.5 mM $CaCl_2$, 1.3 mM $MgCl_2$, 10 mM HEPES and 11 mM glucose. The pH of the solution was adjusted to 7.3 with NaOH. The intracellular recording solution contained 135 mM KCl, 10 mM HEPES, 4 mM $MgCl_2$, 2 mM Na_2-K_2-ATP, 0.2 mM Na_3-GTP and 0.5 mM EGTA. The pH of the solution was adjusted to 7.3 with KOH. Cells were maintained at a holding potential of –60 mV throughout the experiments. Currents were recorded by depolarizing the cells to the desired potential for 400 milliseconds. I-V relationships were obtained by ramp of potential from –120 to +60 mV (360 milliseconds). The resting membrane potential of the cells was measured immediately upon entering the whole-cell recording mode only in cells that did not show sudden increased of leak current when the membrane patch was broken. All experiments were done at room temperature.

We are grateful to F. Soubrier and S. Pons for the gift of the HRE-pGL3-SV40-luciferase construct. We also thank J. Seylaz and H. Petite for their advice on the mesenchymal stem cell cultures. This study was supported by the French Fédération de la Recherche sur le Cerveau (FRC), AMGEN A.S. (U.S.A., France), the French Centre National de la Recherche Scientifique (CNRS) and the French Ministère de l'Education, de la Recherche et de la Technologie.

References

Bertani, N., Malatesta, P., Volpi, G., Sonego, P. and Perris, R. (2005). Neurogenic potential of human mesenchymal stem cells revisited: analysis by immunostaining, time-lapse video and microarray. *J. Cell Sci.* **118**, 3925-3936.

Bito, H., Furuyashiki, T., Ishihara, H., Shibasaki, Y., Ohashi, K., Mizuno, K., Maekawa, M., Ishizaki, T. and Narumiya, S. (2000). A critical role for a Rho-associated kinase, p160ROCK, in determining axon outgrowth in mammalian CNS neurons. *Neuron* **26**, 431-441.

Borlongan, C. V., Tajima, Y., Trojanowski, J. Q., Lee, V. M. and Sanberg, P. R. (1998). Cerebral ischemia and CNS transplantation: differential effects of grafted fetal rat striatal cells and human neurons derived from a clonal cell line. *Neuroreport* **9**, 3703-3709.

Bradbury, A., Possenti, R., Shooter, E. M. and Tirone, F. (1991). Molecular cloning of PC3, a putatively secreted protein whose mRNA is induced by nerve growth factor and depolarization. *Proc. Natl. Acad. Sci. USA* **88**, 3353-3357.

Canzoniere, D., Farioli-Vecchioli, S., Conti, F., Ciotti, M. T., Tata, A. M., Augusti-Tocco, G., Mattei, E., Lakshmana, M. K., Krizhanovsky, V., Reeves, S. A. et al. (2004). Dual control of neurogenesis by PC3 through cell cycle inhibition and induction of Math1. *J. Neurosci.* **24**, 3355-3369.

Cao, L., Jiao, X., Zuzga, D. S., Liu, Y., Fong, D. M., Young, D. and During, M. J. (2004). VEGF links hippocampal activity with neurogenesis, learning and memory. *Nat. Genet.* **36**, 827-835.

Castro, R. F., Jackson, K. A., Goodell, M. A., Robertson, C. S., Liu, H. and Shine, H. D. (2002). Failure of bone marrow cells to transdifferentiate into neural cells in vivo. *Science* **297**, 1299.

Chen, J., Li, Y., Wang, L., Zhang, Z., Lu, D., Lu, M. and Chopp, M. (2001). Therapeutic benefit of intravenous administration of bone marrow stromal cells after cerebral ischemia in rats. *Stroke* **32**, 1005-1011.

Coulet, F., Nadaud, S., Agrapart, M. and Soubrier, F. (2003). Identification of hypoxia-response element in the human endothelial nitric-oxide synthase gene promoter. *J. Biol. Chem.* **278**, 46230-46240.

Csete, M., Rodriguez, L., Wilcox, M. and Chadalavada, S. (2004). Erythropoietin receptor is expressed on adult rat dopaminergic neurons and erythropoietin is neurotrophic in cultured dopaminergic neuroblasts. *Neurosci. Lett.* **359**, 124-126.

Dehmelt, L., Smart, F. M., Ozer, R. S. and Halpain, S. (2003). The role of microtubule-associated protein 2c in the reorganization of microtubules and lamellipodia during neurite initiation. *J. Neurosci.* **23**, 9479-9490.

Deloulme, J. C., Lucas, M., Gaber, C., Bouillon, P., Keller, A., Eclancher, F. and Sensenbrenner, M. (1996). Expression of the neuron-specific enolase gene by rat oligodendroglial cells during their differentiation. *J. Neurochem.* **66**, 936-945.

Dickson, B. J. (2001). Rho GTPases in growth cone guidance. *Curr. Opin. Neurobiol.* **11**, 103-110.

Fabel, K., Tam, B., Kaufer, D., Baiker, A., Simmons, N., Kuo, C. J. and Palmer, T. D. (2003). VEGF is necessary for exercise-induced adult hippocampal neurogenesis. *Eur. J. Neurosci.* **18**, 2803-2812.

Gallo, G. and Letourneau, P. C. (1998). Axon guidance: GTPases help axons reach their targets. *Curr. Biol.* **8**, R80-R82.

Goda, N., Ryan, H. E., Khadivi, B., McNulty, W., Rickert, R. C. and Johnson, R. S. (2003). Hypoxia-inducible factor 1alpha is essential for cell cycle arrest during hypoxia. *Mol. Cell. Biol.* **23**, 359-369.

Guardavaccaro, D., Corrente, G., Covone, F., Micheli, L., D'Agnano, I., Starace, G., Caruso, M. and Tirone, F. (2000). Arrest of G(1)-S progression by the p53-inducible gene PC3 is Rb dependent and relies on the inhibition of cyclin D1 transcription. *Mol. Cell. Biol.* **20**, 1797-1815.

Hall, A. (1998). Rho GTPases and the actin cytoskeleton. *Science* **279**, 509-514.

Hamill, O. P., Marty, A., Neher, E., Sakmann, B. and Sigworth, F. J. (1981). Improved patch-clamp techniques for high-resolution current recording from cells and cell-free membrane patches. *Pflugers Arch.* **391**, 85-100.

Harper, J. W., Adami, G. R., Wei, N., Keyomarsi, K. and Elledge, S. J. (1993). The p21 Cdk-interacting protein Cip1 is a potent inhibitor of G1 cyclin-dependent kinases. *Cell* **75**, 805-816.

Hermann, A., Gastl, R., Liebau, S., Popa, M. O., Fiedler, J., Boehm, B. O., Maisel, M., Lerche, H., Schwarz, J., Brenner, R. et al. (2004). Efficient generation of neural stem cell-like cells from adult human bone marrow stromal cells. *J. Cell Sci.* **117**, 4411-4422.

Hirose, M., Ishizaki, T., Watanabe, N., Uehata, M., Kranenburg, O., Moolenaar, W. H., Matsumura, F., Maekawa, M., Bito, H. and Narumiya, S. (1998). Molecular dissection of the Rho-associated protein kinase (p160ROCK)-regulated neurite remodeling in neuroblastoma N1E-115 cells. *J. Cell Biol.* **141**, 1625-1636.

Huang, Y., Du, K. M., Xue, Z. H., Yan, H., Li, D., Liu, W., Chen, Z., Zhao, Q., Tong, J. H., Zhu, Y. S. et al. (2003). Cobalt chloride and low oxygen tension trigger differentiation of acute myeloid leukemic cells: possible mediation of hypoxia-inducible factor-1alpha. *Leukemia* **17**, 2065-2073.

Hung, S. C., Cheng, H., Pan, C. Y., Tsai, M. J., Kao, L. S. and Ma, H. L. (2002). In vitro differentiation of size-sieved stem cells into electrically active neural cells. *Stem Cells* **20**, 522-529.

Jiang, B. H., Zheng, J. Z., Leung, S. W., Roe, R. and Semenza, G. L. (1997). Transactivation and inhibitory domains of hypoxia-inducible factor 1alpha. Modulation of transcriptional activity by oxygen tension. *J. Biol. Chem.* **272**, 19253-19260.

Jiang, Y., Henderson, D., Blackstad, M., Chen, A., Miller, R. F. and Verfaillie, C. M. (2003). Neuroectodermal differentiation from mouse multipotent adult progenitor cells. *Proc. Natl. Acad. Sci. USA* **100**, 11854-11860.

Jin, K., Zhu, Y., Sun, Y., Mao, X. O., Xie, L. and Greenberg, D. A. (2002). Vascular endothelial growth factor (VEGF) stimulates neurogenesis in vitro and in vivo. *Proc. Natl. Acad. Sci. USA* **99**, 11946-11950.

Kohyama, J., Abe, H., Shimazaki, T., Koizumi, A., Nakashima, K., Gojo, S., Taga, T., Okano, H., Hata, J. and Umezawa, A. (2001). Brain from bone: efficient "meta-differentiation" of marrow stroma-derived mature osteoblasts to neurons with Noggin or a demethylating agent. *Differentiation* **68**, 235-244.

Kong, D., Park, E. J., Stephen, A. G., Calvani, M., Cardellina, J. H., Monks, A., Fisher, R. J., Shoemaker, R. H. and Melillo, G. (2005). Echinomycin, a small-molecule inhibitor of hypoxia-inducible factor-1 DNA-binding activity. *Cancer Res.* **65**, 9047-9055.

Kopen, G. C., Prockop, D. J. and Phinney, D. G. (1999). Marrow stromal cells migrate throughout forebrain and cerebellum, and they differentiate into astrocytes after injection into neonatal mouse brains. *Proc. Natl. Acad. Sci. USA* **96**, 10711-10716.

Kotake-Nara, E., Takizawa, S., Quan, J., Wang, H. and Saida, K. (2005). Cobalt chloride induces neurite outgrowth in rat pheochromocytoma PC-12 cells through regulation of endothelin-2/vasoactive intestinal contractor. *J. Neurosci. Res.* **81**, 563-571.

Krause, D. S. (2002). Plasticity of marrow-derived stem cells. *Gene Ther.* **9**, 754-758.

Kurozumi, K., Nakamura, K., Tamiya, T., Kawano, Y., Ishii, K., Kobune, M., Hirai, S., Uchida, H., Sasaki, K., Ito, Y. et al. (2005). Mesenchymal stem cells that produce neurotrophic factors reduce ischemic damage in the rat middle cerebral artery occlusion model. *Mol. Ther.* **11**, 96-104.

Lee, S. G., Lee, H. and Rho, H. M. (2001). Transcriptional repression of the human p53 gene by cobalt chloride mimicking hypoxia. *FEBS Lett.* **507**, 259-263.

Lendahl, U., Zimmerman, L. B. and McKay, R. D. (1990). CNS stem cells express a new class of intermediate filament protein. *Cell* **60**, 585-595.

Long, Y. and Yang, K. Y. (2003). Bone marrow derived cells for brain repair: recent findings and current controversies. *Curr. Mol. Med.* **3**, 719-725.

Lu, P., Blesch, A. and Tuszynski, M. H. (2004). Induction of bone marrow stromal cells to neurons: differentiation, transdifferentiation, or artifact? *J. Neurosci. Res.* **77**, 174-191.

Luo, L. (2000). Rho GTPases in neuronal morphogenesis. *Nat. Rev. Neurosci.* **1**, 173-180.

Mahmood, A., Lu, D., Wang, L., Li, Y., Lu, M. and Chopp, M. (2001). Treatment of traumatic brain injury in female rats with intravenous administration of bone marrow stromal cells. *Neurosurgery* **49**, 1196-1204.

Mammoto, A., Huang, S., Moore, K., Oh, P. and Ingber, D. E. (2004). Role of RhoA, mDia, and ROCK in cell shape-dependent control of the Skp2-p27kip1 pathway and the G1/S transition. *J. Biol. Chem.* **279**, 26323-26330.

McBeath, R., Pirone, D. M., Nelson, C. M., Bhadriraju, K. and Chen, C. S. (2004). Cell shape, cytoskeletal tension, and RhoA regulate stem cell lineage commitment. *Dev. Cell* **6**, 483-495.

Narumiya, S., Ishizaki, T. and Watanabe, N. (1997). Rho effectors and reorganization of actin cytoskeleton. *FEBS Lett.* **410**, 68-72.

Neuhuber, B., Gallo, G., Howard, L., Kostura, L., Mackay, A. and Fischer, I. (2004). Reevaluation of in vitro differentiation protocols for bone marrow stromal cells: disruption of actin cytoskeleton induces rapid morphological changes and mimics neuronal phenotype. *J. Neurosci. Res.* **77**, 192-204.

Nikolic, M. (2002). The role of Rho GTPases and associated kinases in regulating neurite outgrowth. *Int. J. Biochem. Cell Biol.* **34**, 731-745.

Padovan, C. S., Jahn, K., Birnbaum, T., Reich, P., Sostak, P., Strupp, M. and Straube, A. (2003). Expression of neuronal markers in differentiated marrow stromal cells and CD133+ stem-like cells. *Cell Transplant.* **12**, 839-848.

Pittenger, M. F., Mackay, A. M., Beck, S. C., Jaiswal, R. K., Douglas, R., Mosca, J. D., Moorman, M. A., Simonetti, D. W., Craig, S. and Marshak, D. R. (1999). Multilineage potential of adult human mesenchymal stem cells. *Science* **284**, 143-147.

Salim, A., Nacamuli, R. P., Morgan, E. F., Giaccia, A. J. and Longaker, M. T. (2004). Transient changes in oxygen tension inhibit osteogenic differentiation and Runx2 expression in osteoblasts. *J. Biol. Chem.* **279**, 40007-40016.

Sanchez-Ramos, J. R. (2002). Neural cells derived from adult bone marrow and umbilical cord blood. *J. Neurosci. Res.* **69**, 880-893.

Sanchez-Ramos, J., Song, S., Cardozo-Pelaez, F., Hazzi, C., Stedeford, T., Willing, A., Freeman, T. B., Saporta, S., Janssen, W., Patel, N. et al. (2000). Adult bone marrow stromal cells differentiate into neural cells in vitro. *Exp. Neurol.* **164**, 247-256.

Semenza, G. L. (2000). Oxygen-regulated transcription factors and their role in pulmonary disease. *Respir. Res.* **1**, 159-162.

Sensenbrenner, M., Lucas, M. and Deloulme, J. C. (1997). Expression of two neuronal markers, growth-associated protein 43 and neuron-specific enolase, in rat glial cells. *J. Mol. Med.* **75**, 653-663.

Sharp, F. R. and Bernaudin, M. (2004). HIF1 and oxygen sensing in the brain. *Nat. Rev. Neurosci.* **5**, 437-448.

Shen, Q., Goderie, S. K., Jin, L., Karanth, N., Sun, Y., Abramova, N., Vincent, P., Pumiglia, K. and Temple, S. (2004). Endothelial cells stimulate self-renewal and expand neurogenesis of neural stem cells. *Science* **304**, 1338-1340.

Shingo, T., Sorokan, S. T., Shimazaki, T. and Weiss, S. (2001). Erythropoietin regulates the in vitro and in vivo production of neuronal progenitors by mammalian forebrain neural stem cells. *J. Neurosci.* **21**, 9733-9743.

Studer, L., Tabar, V. and McKay, R. D. (1998). Transplantation of expanded mesencephalic precursors leads to recovery in parkinsonian rats. *Nat. Neurosci.* **1**, 290-295.

Studer, L., Csete, M., Lee, S. H., Kabbani, N., Walikonis, J., Wold, B. and McKay, R. (2000). Enhanced proliferation, survival, and dopaminergic differentiation of CNS precursors in lowered oxygen. *J. Neurosci.* **20**, 7377-7383.

Sun, Y., Jin, K., Xie, L., Childs, J., Mao, X. O., Logvinova, A. and Greenberg, D. A. (2003). VEGF-induced neuroprotection, neurogenesis, and angiogenesis after focal cerebral ischemia. *J. Clin. Invest.* **111**, 1843-1851.

Tomita, S., Ueno, M., Sakamoto, M., Kitahama, Y., Ueki, M., Maekawa, N., Sakamoto, H., Gassmann, M., Kageyama, R., Ueda, N. et al. (2003). Defective brain development in mice lacking the Hif-1alpha gene in neural cells. *Mol. Cell. Biol.* **23**, 6739-6749.

Tondreau, T., Lagneaux, L., Dejeneffe, M., Massy, M., Mortier, C., Delforge, A. and Bron, D. (2004). Bone marrow-derived mesenchymal stem cells already express specific neural proteins before any differentiation. *Differentiation* **72**, 319-326.

Tropepe, V., Hitoshi, S., Sirard, C., Mak, T. W., Rossant, J. and van der Kooy, D. (2001). Direct neural fate specification from embryonic stem cells: a primitive mammalian neural stem cell stage acquired through a default mechanism. *Neuron* **30**, 65-78.

Vallieres, L. and Sawchenko, P. E. (2003). Bone marrow-derived cells that populate the adult mouse brain preserve their hematopoietic identity. *J. Neurosci.* **23**, 5197-5207.

Wang, G. L. and Semenza, G. L. (1993). Desferrioxamine induces erythropoietin gene expression and hypoxia-inducible factor 1 DNA-binding activity: implications for models of hypoxia signal transduction. *Blood* **82**, 3610-3615.

Wang, G., Hazra, T. K., Mitra, S., Lee, H. M. and Englander, E. W. (2000). Mitochondrial DNA damage and a hypoxic response are induced by CoCl(2) in rat neuronal PC12 cells. *Nucleic Acids Res.* **28**, 2135-2140.

Wang, G., Woods, A., Sabari, S., Pagnotta, L., Stanton, L. A. and Beier, F. (2004). RhoA/ROCK signaling suppresses hypertrophic chondrocyte differentiation. *J. Biol. Chem.* **279**, 13205-13214.

Wang, L., Zhang, Z., Wang, Y., Zhang, R. and Chopp, M. (2004). Treatment of stroke with erythropoietin enhances neurogenesis and angiogenesis and improves neurological function in rats. *Stroke* **35**, 1732-1737.

Wislet-Gendebien, S., Leprince, P., Moonen, G. and Rogister, B. (2003). Regulation of neural markers nestin and GFAP expression by cultivated bone marrow stromal cells. *J. Cell Sci.* **116**, 3295-3302.

Wislet-Gendebien, S., Hans, G., Leprince, P., Rigo, J. M., Moonen, G. and Rogister, B. (2005a). Plasticity of cultured mesenchymal stem cells: switch from nestin-positive to excitable neuron-like phenotype. *Stem Cells* **23**, 392-402.

Wislet-Gendebien, S., Wautier, F., Leprince, P. and Rogister, B. (2005b). Astrocytic and neuronal fate of mesenchymal stem cells expressing nestin. *Brain Res. Bull.* **68**, 95-102.

Woodbury, D., Schwarz, E. J., Prockop, D. J. and Black, I. B. (2000). Adult rat and human bone marrow stromal cells differentiate into neurons. *J. Neurosci. Res.* **61**, 364-370.

Xiong, Y., Hannon, G. J., Zhang, H., Casso, D., Kobayashi, R. and Beach, D. (1993). p21 is a universal inhibitor of cyclin kinases. *Nature* **366**, 701-704.

Yu, X., Shacka, J. J., Eells, J. B., Suarez-Quian, C., Przygodzki, R. M., Beleslin-Cokic, B., Lin, C. S., Nikodem, V. M., Hempstead, B., Flanders, K. C. et al. (2002). Erythropoietin receptor signalling is required for normal brain development. *Development* **129**, 505-516.

Zhu, Y., Jin, K., Mao, X. O. and Greenberg, D. A. (2003). Vascular endothelial growth factor promotes proliferation of cortical neuron precursors by regulating E2F expression. *FASEB J.* **17**, 186-193.